



HAL
open science

Homogeneity-Based Control Strategy for Trajectory Tracking in Perturbed Unicycle Mobile Robots

Yu Zhou, Héctor Ríos, Manuel Mera, Andrey Polyakov, Gang Zheng, Alejandro Dzul

► **To cite this version:**

Yu Zhou, Héctor Ríos, Manuel Mera, Andrey Polyakov, Gang Zheng, et al.. Homogeneity-Based Control Strategy for Trajectory Tracking in Perturbed Unicycle Mobile Robots. *IEEE Transactions on Control Systems Technology*, 2024, 32 (1), pp.274-281. 10.1109/TCST.2023.3300273 . hal-04390587

HAL Id: hal-04390587

<https://hal.science/hal-04390587v1>

Submitted on 12 Jan 2024

HAL is a multi-disciplinary open access archive for the deposit and dissemination of scientific research documents, whether they are published or not. The documents may come from teaching and research institutions in France or abroad, or from public or private research centers.

L'archive ouverte pluridisciplinaire **HAL**, est destinée au dépôt et à la diffusion de documents scientifiques de niveau recherche, publiés ou non, émanant des établissements d'enseignement et de recherche français ou étrangers, des laboratoires publics ou privés.

Homogeneity-based Control Strategy for Trajectory Tracking in Perturbed Unicycle Mobile Robots

Y. Zhou¹, H. Ríos^{2,†}, M. Mera³, A. Polyakov¹, G. Zheng¹ and A. Dzul²

Abstract—This paper deals with the tracking problem for the Unicycle Mobile Robot (UMR) with slippage effects. A homogeneous controller is developed based on a particular cascade control strategy. The robustness of the closed-loop system is studied. The design is essentially based on the canonical homogeneous norm being a Lyapunov function of the system. The (finite-time or exponential) convergence rate of the homogeneous controller can be tuned by a proper selection of the so-called homogeneity degree. Some experimental results illustrate the performance of the proposed homogeneous control in the UMR QBot2 by Quanser.

Index Terms—Unicycle Mobile Robots, Trajectory Tracking, Homogeneity, Finite-Time.

I. INTRODUCTION

A wheeled mobile robot, which has no conventional centred orientable wheels and two conventional fixed wheels, is referred to as a mobile robot of Type (2,0) or a UMR (see, *e.g.*, [1]). The unicycle kinematic model, which is often considered to be a disturbance-free system, can be affected by wheel slippage and sliding, leading to unmatched additive input-dependent disturbances in the velocity channels [2]. Several control algorithms have been developed in the past decade to address this issue, including adaptive control [3], [4] and disturbance observer-based regulation [5]. However, these methods rely on a dynamic model of the system and acceleration control, which may not always be available. Sliding-mode control [6], [7] is a common approach but can suffer from the chattering problem, which can degrade control precision. Model predictive control [8] is computationally demanding and may involve non-admissible jumps in control inputs.

The homogeneity is a dilation symmetry (see, *e.g.*, [9], [10], [11] and [12]), which is widely utilized for the UMR control design in both discontinuous (see, *e.g.*, [13] and [14]) and time-varying approaches (see, *e.g.*, [15], [16], [17] and [18]). Compared to linear systems, homogeneous systems have some important properties such as faster convergence, better robustness and fewer overshoots (for more details, see [9], [10], [11] and [12]). One of the distinguishing features of a homogeneous system is that its convergence rate is determined by its homogeneity degree.

¹Univ. Lille, Inria, CNRS, Centrale Lille, France, E-mails: yu.zhou (andrey.polyakov, gang.zheng)@inria.fr

²Tecnológico Nacional de México/I.T. La Laguna, C.P. 27000, Torreón, Coahuila, México. Emails: hriosb(aedzull)@correo.itlalaguna.edu.mx

[†]CONACYT IxM, C.P. 03940, Mexico City, México.

³Instituto Politécnico Nacional, ESIME Ticomán, C.P. 07340, Mexico City, México. Email: mmerah@ipn.mx

The finite-time control for the UMR has attracted a lot of attention in recent decades due to its fast convergence and robustness properties. Some finite-time controllers have been designed based on homogeneity since any asymptotically stable homogeneous system with a negative degree is finite-time stable [10]. Various finite-time homogeneous control algorithms for UMR are developed (see, *e.g.*, [19], [20], [21], [22] and [23]). In [21], [22], and [23], homogeneity-based algorithms for the finite-time trajectory-tracking problem are investigated using a cascade structure. However, these algorithms require a nonzero desired angular velocity, therefore they are unable to track some trajectories, *e.g.*, a simple straight line. In addition, none of them deals with perturbed kinematic models.

For the trajectory-tracking control problem, overshoots and robustness are two of the most crucial performance metrics. However, classic asymptotic tracking control with a constant gain fails to account for both metrics. The classic discontinuous sliding-mode control approach can provide bounded control signals and strong robustness but it produces chattering. In contrast, the homogeneous control approach can be continuous and offers a potential solution for balancing the trade-off between overshooting and robustness. In this sense, the aim of this paper is to develop a homogeneity-based control strategy to solve the trajectory-tracking problem for a UMR taking into account the perturbed kinematic model. The homogeneous control design is based on the so-called canonical homogeneous norm (see [24] and [25]) allowing simple rules to tune the control parameters. Considering the under-actuated characteristic of the system, we propose a cascade control scheme. *The main contribution is threefold:* 1) The trajectory-tracking problem in UMRs is solved based on novel generalized homogeneous controllers allowing both asymptotic and finite-time stabilization of the tracking error dynamics. The proposed cascade control scheme allows tracking of a wider range of trajectories. 2) Input-to-State Stability (ISS) with respect to a class of perturbations is proven. A strategy of control parameters tuning, allowing improvement of robustness and control precision, is proposed as well. 3) The proposed homogeneous control is evaluated through real-time experiments with the UMR QBot2 by Quanser. Compared to classic asymptotic and sliding-mode controllers, it achieves better performance in balancing overshoot and disturbance rejection. Fig. 1 illustrates the proposed solution.

A preliminary version of this paper was presented at [26]. The main differences with respect to this paper are: perturbations caused by slippage are considered; a new

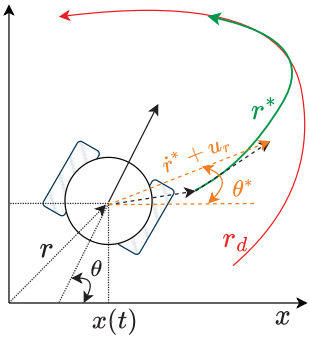


Fig. 1: Schematic Solution. This figure highlights that in the case of a large initial error, a nominal trajectory $[r^*, \theta^*]$ may be employed to guide the system toward the desired trajectory $[r_d, \theta_d]$.

control design is proposed, allowing better tuning under perturbations; formal proofs of the results are provided; and experimental validation together with comparisons are provided.

The paper is structured as follows: Section II presents the problem statement, Section III recalls useful results about homogeneous systems, and Section IV contains the main results of the research, including cascade system design, homogeneous control design, and stability/robustness analysis. Section V discusses experimental results using a QBot2, and Section VI presents concluding remarks. Supporting results and remarks are provided in the Appendix.

Notation: Let \mathbb{R} be the set of real numbers, $\mathbb{R}_+ = \{\alpha \in \mathbb{R} : \alpha \geq 0\}$; $\|\cdot\|$ be a norm in \mathbb{R}^n , $\mathbf{0}$ denotes the zero vector from \mathbb{R}^n ; $P \succ 0$ ($\prec 0, \succeq 0, \preceq 0$) for $P \in \mathbb{R}^{n \times n}$ means that the matrix P is symmetric and positive (negative) definite (semidefinite); $\lambda_{\min}(P)$ and $\lambda_{\max}(P)$ represent the minimal and maximal eigenvalue of a matrix $P = P^\top$; for $P \succeq 0$ the square root of P is a matrix $M = P^{\frac{1}{2}}$ such that $M^2 = P$. The canonical Euclidean norm for $x \in \mathbb{R}^n$ is denoted as $\|x\|_2 = \sqrt{x^\top x}$. Let denote by \mathcal{K} the set of continuous increasing functions map $\mathbb{R}_+ \rightarrow \mathbb{R}_+$. The set of unbounded \mathcal{K} functions is denoted by \mathcal{K}_∞ . Let continuous function $\beta(\cdot, \cdot) \in \mathcal{KL}$ if it is \mathcal{K} with respect to the first argument and strictly decreasing to zero with respect to the second argument. The term L^∞ is the set of the essentially bounded measurable functions while L^1_{loc} is the set of local Lebesgue measure functions.

II. PROBLEM STATEMENT

Let us consider the kinematic model of a UMR with disturbances [2]:

$$\begin{cases} \dot{r} = (1 + d_1(t))v\xi, & r(0) = r_0, \\ \dot{\theta} = (1 + d_2(t))\omega, & \theta(0) = \theta_0, \end{cases} \quad (1)$$

where $r = [x, y]^\top \in \mathbb{R}^2$ is the planar position vector, $v \in \mathbb{R}_+$ is the velocity magnitude, $\xi = [\cos(\theta), \sin(\theta)]^\top$ is the unit vector that defines the direction of the velocity, $\theta \in \mathbb{R}$ is the angle between the vector r and the x -axis, $\omega \in \mathbb{R}$ is

the angular velocity. The terms d_1 and d_2 represent some time-varying perturbations, which are multiplicative to the inputs. They model slipping effects of the wheels [2]. It is assumed that the perturbations are unknown but bounded: $-1 < -\hat{d}_i \leq d_i(t) \leq \hat{d}_i < 1$, $i = 1, 2$, with some known constants \hat{d}_1 and \hat{d}_2 . Note that the constraint $\hat{d}_i < 1$ ensures that the perturbations do not change a sign in the control input. We assume that x, y and θ are the only available measurements of the system.

The system is unable to track any arbitrary trajectory due to the non-holonomic constraint $\dot{x} \sin(\theta) - \dot{y} \cos(\theta) = 0$. So, we define a *feasible trajectory* for the system (1) as a pair $r_d \in C^2(\mathbb{R}_+, \mathbb{R}^2)$, $\theta_d \in C^2(\mathbb{R}_+, \mathbb{R})$, satisfying $\dot{r}_d = v_d \xi_d$ and $\dot{x}_d \sin(\theta_d) - \dot{y}_d \cos(\theta_d) = 0$, with $r_d = [x_d, y_d]^\top$, $\xi_d = [\cos(\theta_d), \sin(\theta_d)]^\top$ and some $v_d \in C^1(\mathbb{R}_+, \mathbb{R}_+)$ being a desired velocity.

The conventional trajectory-tracking problem for the perturbation-free system (1) can be formulated as follows: *design a control law, i.e., v and ω , such that, for any desired feasible trajectory $[r_d, \theta_d]$, $\|r(t) - r_d(t)\|_2 \rightarrow 0$ and $|\theta(t) - \theta_d(t)| \rightarrow 0$ hold as $t \rightarrow \infty$.*

In particular, we investigate the possibility of homogeneous finite-time¹ stabilization of the error dynamics as well as the robustness of the control system in the sense of ISS, with respect to the perturbations d_1 and d_2 .

III. PRELIMINARIES

The homogeneity (dilation symmetry) based analysis and design of the control system require a dilation to be specified. By definition, a dilation $\mathbf{d}(s)$, with $s \in \mathbb{R}$, is a one-parameter group of transformations satisfying the limit property $\lim_{s \rightarrow s^\infty} \|\mathbf{d}(s)x\| = e^{s^\infty}$, with $s^\infty = \pm\infty$, for all $x \neq \mathbf{0}$ [28]. The linear dilation in \mathbb{R}^n is defined as in [25], i.e., $\mathbf{d}(s) = e^{sG_d} := \sum_{i=0}^{+\infty} \frac{s^i G_d^i}{i!}$, $s \in \mathbb{R}$, where $G_d \in \mathbb{R}^{n \times n}$ is an anti-Hurwitz² matrix called the generator of the dilation \mathbf{d} .

Definition 1: [27]. A vector field $f : \mathbb{R}^n \rightarrow \mathbb{R}^n$ (resp., a function $h : \mathbb{R}^n \rightarrow \mathbb{R}$) is said to be \mathbf{d} -homogeneous of degree $\mu \in \mathbb{R}$ if $f(\mathbf{d}(s)) = e^{\mu s} \mathbf{d}(s) f(x)$ (resp., $h(\mathbf{d}(s)) = e^{\mu s} h(x)$), $\forall x \in \mathbb{R}^n$, $\forall s \in \mathbb{R}$, where \mathbf{d} is a linear dilation in \mathbb{R}^n .

The set of solutions of a system with a homogeneous right-hand side is homogeneous, and any asymptotically stable system has a homogeneous Lyapunov function in the view of Zubov-Rosier Theorem (see, e.g., [27] and [29]).

Definition 2: [25]. The function $\|\cdot\|_d : \mathbb{R}^n \rightarrow \mathbb{R}_+$, defined as $\|\mathbf{0}\|_d = 0$ and $\|u\|_d = e^{s u}$, where $s_u \in \mathbb{R} : \|\mathbf{d}(-s_u)u\| = 1$, is called the canonical \mathbf{d} -homogeneous norm in \mathbb{R}^n , where \mathbf{d} is a linear monotone dilation³.

¹The system $\dot{e} = f(t, e)$, $t > t_0$ is globally uniformly finite-time stable if it is uniformly Lyapunov stable and there exists a locally bounded function $T : \mathbb{R}^n \rightarrow \mathbb{R}_+$ such that $\forall e_0 \in \mathbb{R}^n$, $e(t_0) = e_0 \Rightarrow e(t) = \mathbf{0}$, $\forall t \geq t_0 + T(e_0)$ [27].

²A matrix G_d is anti-Hurwitz if $-G_d$ is Hurwitz [12].

³A dilation $\mathbf{d}(s)$ in \mathbb{R}^n is monotone if the function $s \mapsto \|\mathbf{d}(s)x\|$ is strictly monotone for any $x \neq \mathbf{0}$. Any linear dilation in \mathbb{R}^n is strictly monotone under a proper selection of a weighted Euclidean norm [25].

The canonical homogeneous norm is induced by a (usual) norm in \mathbb{R}^n . Notice that if $\|\cdot\| \in C^1(\mathbb{R}^n \setminus \{\mathbf{0}\})$ then $\|\cdot\|_d \in C^1(\mathbb{R}^n \setminus \{\mathbf{0}\})$, in particular, we have [25]

$$\frac{\partial \|x\|_d}{\partial x} = \|x\|_d \frac{x^\top d^\top (-\ln \|x\|_d) P d (-\ln \|x\|_d)}{x^\top d^\top (-\ln \|x\|_d) P G_d d (-\ln \|x\|_d) x}, \quad (2)$$

for $x \neq \mathbf{0}$, provided that $\|x\|_d$ is the canonical homogeneous norm induced by the norm $\|x\| = \sqrt{x^\top P x}$, with $P = P^\top \in \mathbb{R}^{n \times n}$ satisfying: $P G_d + G_d^\top P \succ 0$ and $P \succ 0$.

IV. HOMOGENEITY-BASED CONTROL FOR THE UMR

A. Cascade Control Design for the Perturbation-free Case

The main aim of this paper is to develop a control strategy that solves the trajectory tracking problem for the UMR being an under-actuated system. This section presents a cascade control paradigm that simplifies the design.

Let us define the tracking errors as

$$e_r = r - r^*, \quad e_\theta = \theta - \theta^*, \quad (3)$$

where r^* is a virtual trajectory and θ^* is an orientation angle to be designed such that $\theta^* \rightarrow \theta_d$ as $e_r \rightarrow 0$ and $r^* \rightarrow r_d$ as $t \rightarrow +\infty$. Then, the tracking error system is given by:

$$\dot{e}_r = (1 + d_1)v\xi - \dot{r}^*, \quad \dot{e}_\theta = (1 + d_2)\omega - \dot{\theta}^*. \quad (4)$$

The idea of the cascade structure is that the position subsystem determines the desired velocity vector $v\xi^*$; v is the actual input of the system, then the direction command ξ^* is tracked by the orientation subsystem. Following the backstepping ideas, we assume that there exist virtual controllers u_r and u_θ dependent on e_r and e_θ , which stabilize the error subsystems $\dot{e}_r = u_r$ and $\dot{e}_\theta = u_\theta$ (at least in the disturbance-free case). In this case, we rewrite the error dynamics as

$$\begin{cases} \dot{e}_r = u_r + \delta_1, \\ \dot{e}_\theta = u_\theta + \delta_2, \end{cases} \quad (5)$$

where $\delta_1 = (1 + d_1)v\xi - \dot{r}^* - u_r$ and $\delta_2 = (1 + d_2)\omega - \dot{\theta}^* - u_\theta$. Therefore, to stabilize the error vector e_r , we need to define the control inputs v and ω such that $\delta = (\delta_1, \delta_2)^\top \rightarrow 0$, at least, for $d_1 = d_2 = 0$. Due to the under-actuated nature of the system, this cannot be done for position and orientation subsystems independently.

Let us select the control inputs as follows:

$$v = \|\dot{r}^* + u_r\|_2, \quad \omega = \omega^* + u_\theta, \quad (6)$$

where

$$\omega^* := \frac{(\dot{r}^* + u_r)^\top \begin{bmatrix} 0 & -1 \\ 1 & 0 \end{bmatrix} \frac{d(\dot{r}^* + u_r)}{dt}}{\|\dot{r}^* + u_r\|_2^2}. \quad (7)$$

Then, the following lemma provides some properties of the signals r^* and θ^* .

Lemma 1: *Let the functions $t \mapsto \dot{r}^*(t)$ and $t \mapsto u_r(t)$ be continuously differentiable on \mathbb{R}_+ , the function $t \mapsto \omega^*(t)$ be locally Lebesgue integrable, the set $\Delta = \{t \in \mathbb{R}_+ : \dot{r}^*(t) + u_r(t) = \mathbf{0}\}$, be finite and $0 \notin \Delta$. Then:*

- The differential equation

$$\dot{\theta}^* = \omega^*, \quad \theta_0^* = \arctan \left(\frac{\begin{bmatrix} 0 & 1 \\ 1 & 0 \end{bmatrix} (\dot{r}_0^* + u_{r0})}{\begin{bmatrix} 1 & 0 \\ 1 & 0 \end{bmatrix} (\dot{r}_0^* + u_{r0})} \right), \quad (8)$$

where r_0^* and u_{r0} denote the values of r^* and u_r at the initial instant of time $t = 0$, has the unique solution $t \mapsto \theta^*(t)$ satisfying

$$\theta^*(t) = \theta_0^* + \int_0^t \omega^*(\tau) d\tau, \quad t \in \mathbb{R}_+, \quad (9)$$

that is absolutely continuous on \mathbb{R}_+ and continuously differentiable on $\mathbb{R}_+ \setminus \{\Delta\}$;

- The vector-valued function $t \mapsto \xi^*(t) := \begin{bmatrix} \cos(\theta^*(t)) \\ \sin(\theta^*(t)) \end{bmatrix}$, satisfies the identity: $\xi^*(t) = \frac{\dot{r}^*(t) + u_r(t)}{\|\dot{r}^*(t) + u_r(t)\|_2}$, $\forall t \in \mathbb{R}_+$;
- The function $t \mapsto e_\theta(t)$ is absolutely continuous on \mathbb{R}_+ , provided that ω is locally Lebesgue integrable.

Proof: Since \dot{r}^* and u_r are continuously differentiable functions of time then ω^* is continuous on $\mathbb{R}^n \setminus \Delta$. In this case, the Lebesgue integrability of ω^* and finiteness of Δ imply that the differential equation (8) has a unique Caratheodory solution given by (9) (see, e.g., [29]).

Let us denote $\tilde{\xi}(t) := \frac{\dot{r}^*(t) + u_r(t)}{\|\dot{r}^*(t) + u_r(t)\|_2}$. Since $\tilde{\xi}(t) \in \mathbb{R}^2$ is a unit vector for $t \notin \Delta$; then, there exists a function $t \mapsto \tilde{\theta}(t)$ such that

$$\begin{aligned} \cos(\tilde{\theta}(t)) &= \frac{\begin{bmatrix} 1 & 0 \\ 1 & 0 \end{bmatrix} (\dot{r}^*(t) + u_r(t))}{\|\dot{r}^*(t) + u_r(t)\|_2}, \quad \sin(\tilde{\theta}(t)) = \frac{\begin{bmatrix} 0 & 1 \\ 1 & 0 \end{bmatrix} (\dot{r}^*(t) + u_r(t))}{\|\dot{r}^*(t) + u_r(t)\|_2}, \\ \tilde{\theta}_0 &= \arctan \left(\frac{\begin{bmatrix} 0 & 1 \\ 1 & 0 \end{bmatrix} (\dot{r}_0^* + u_{r0})}{\begin{bmatrix} 1 & 0 \\ 1 & 0 \end{bmatrix} (\dot{r}_0^* + u_{r0})} \right). \end{aligned}$$

Note that the function $\tilde{\theta}$ satisfying the latter identities is not unique but it is differentiable at any $t \notin \Delta$ and $\frac{d\tilde{\xi}(t)}{dt} = \dot{\theta}(t) \begin{bmatrix} 0 & 1 \\ -1 & 0 \end{bmatrix} \tilde{\xi}(t)$.

Hence, we derive $\dot{\theta}(t) = \tilde{\xi}^\top(t) \begin{bmatrix} 0 & -1 \\ 1 & 0 \end{bmatrix} \frac{d\tilde{\xi}(t)}{dt}$ and

$$\dot{\theta}(t) = \frac{(\dot{r}^*(t) + u_r(t))^\top \begin{bmatrix} 0 & -1 \\ 1 & 0 \end{bmatrix} \frac{d(\dot{r}^*(t) + u_r(t))}{dt}}{\|\dot{r}^*(t) + u_r(t)\|_2}.$$

Since $\theta_0^* = \tilde{\theta}_0$ and $\frac{d\tilde{\theta}(t)}{dt} = \dot{\theta}^*(t)$, almost on every $t \in \mathbb{R}_+$; then, taking into account integrability of ω^* , $\tilde{\theta}$ can always be selected such that $\theta^*(t) = \tilde{\theta}(t)$, $\forall t \in \mathbb{R}_+$.

If the conditions of Lemma 1 are fulfilled, and v and ω are defined as in (6); then, the set Δ defines some instances of time, where $\dot{\theta}^*$ has a singularity. In this case, the error equation (5) is fulfilled almost everywhere with

$$\delta_1 = \|\dot{r}^* + u_r\| \left((1 + d_1)\xi - \xi^* \right), \quad \delta_2 = d_2(u_\theta + \omega^*),$$

and due to $\|\xi\| = 1$, it follows that

$$\xi - \xi^* = \begin{bmatrix} \cos(\theta) - \cos(\theta^*) \\ \sin(\theta) - \sin(\theta^*) \end{bmatrix} = 2 \sin\left(\frac{e_\theta}{2}\right) \begin{bmatrix} -\sin((\theta + \theta^*)/2) \\ \cos((\theta + \theta^*)/2) \end{bmatrix},$$

and then, we have

$$\|\delta_1\|_2 \leq \|\dot{r}^* + u_r\|_2 (2 |\sin(e_\theta/2)| + |d_1|), \quad (10)$$

for almost all $t \in \mathbb{R}_+$. Since $e_\theta = \theta - \theta^*$, the locally Lebesgue integrable functions ω and ω^* indicate the absolute continuity of e_θ . ■

Remark 1: *Note that θ^* is defined by (9) just for simplicity of the mathematical constructions and proofs. Since $\theta_0^* = \tilde{\theta}_0$ and $d\tilde{\theta}(t)/dt = \dot{\theta}^*(t)$, for almost every t on \mathbb{R}_+ ; then, in practice, a computation of $\theta^*(t)$ can be realized by using:*

$$\theta^*(t) = \arctan \left(\frac{\begin{bmatrix} 0 & 1 \\ 1 & 0 \end{bmatrix} (\dot{r}^*(t) + u_r(t))}{\begin{bmatrix} 1 & 0 \\ 1 & 0 \end{bmatrix} (\dot{r}^*(t) + u_r(t))} \right). \quad (11)$$

From a theoretical point of view, a virtual trajectory r^* should be selected such that ω^* has no singular points. In practice, we set $r^* = r_d$ since the set $\{t \in \mathbb{R}_+ : u_r(t) = -\dot{r}_d(t) \neq \mathbf{0}\}$ does not contain any equilibrium of system; then, for any feasible trajectory, the set of such time instances usually has the zero measure.

In the absence of disturbances ($d_1 = d_2 = 0$), one has that $\delta \rightarrow 0$ as $e_\theta \rightarrow 0$. However, δ may be non-vanishing in the general case; then, we use below the generalized homogeneity to analyse the robustness of the control system with respect to disturbances. In the following section, we show that u_r and u_θ can always be selected such that the error dynamics of the system (5) is locally homogeneous in a certain sense.

B. Locally Homogeneous Tracking Error Dynamics

Based on the scheme described in the previous subsection, we construct a homogeneous cascade system in this section. The orientation command (7) calls for the derivative of u_r . To guarantee the continuous differentiability of u_r , let us define the virtual control u_r as

$$u_r = u, \quad (12)$$

$$\dot{u} = u_{hom}(\zeta) := \|\zeta\|_{\mathbf{d}}^{1+\mu} K \mathbf{d} (-\ln \|\zeta\|_{\mathbf{d}}) \zeta, \quad (13)$$

where $\zeta = [e_r^\top, u^\top]^\top$, $\mu \in [-1, 1/2]$ and $K = [-k_1 I_2, -k_2 I_2]$, with some positive gains $k_1, k_2 > 0$. The dilation, in \mathbb{R}^4 , \mathbf{d} is generated by $G_{\mathbf{d}} = \text{diag}((1-\mu)I_2, I_2)$, and the canonical homogeneous norm $\|\cdot\|_{\mathbf{d}}$ is induced by the norm $\|\zeta\| = \sqrt{\zeta^\top P \zeta}$, and $P = \begin{bmatrix} k_1 I_2 & \varepsilon I_2 \\ \varepsilon I_2 & I_2 \end{bmatrix}$, with some positive $\varepsilon > 0$.

Let the virtual control of the orientation be defined as

$$u_\theta = -\alpha |e_\theta|^\nu e_\theta, \quad \alpha > 0, \quad \nu \geq -1. \quad (14)$$

The closed-loop system can be represented as follows

$$\dot{\eta} = f(\eta) + \delta, \quad (15)$$

$$f(\eta) := [f_1^\top(\zeta) \quad f_2^\top(e_\theta)]^\top,$$

$$f_1(\zeta) = A\zeta + B u_{hom}(\zeta), \quad f_2(e_\theta) = u_\theta(e_\theta),$$

where $\delta = [\delta_1^\top, \mathbf{0}, \delta_2^\top]^\top$ and $\eta = [\zeta^\top, e_\theta]^\top$. Notice that the vector field f is homogeneous. Indeed, the vector field f_1 is \mathbf{d} -homogeneous of degree μ . The vector field f_2 is e^ν -homogeneous of degree ν . If $\nu > 0$ or $\nu = \mu = 0$, then the vector field f is \mathbf{d} -homogeneous of degree μ for the dilation in \mathbb{R}^5 , defined as $\mathbf{d}(s) = \text{diag}(\mathbf{d}(s), e^{\gamma s})$, where $\gamma = \frac{\mu}{\nu}$, for $\nu \neq 0$; and $\gamma = 1$, for $\nu = 0$. Simple computations show that $f(\mathbf{d}(s)\eta) = e^{\mu s} \mathbf{d}(s) f(\eta)$, for all $\eta \in \mathbb{R}^5$, $\forall s \in \mathbb{R}$. Therefore, the system (15) can be regarded as a homogeneous system with perturbations. However, the term δ depends on the subsystem states, and the unknown disturbance d_1 and d_2 . The stability and robustness of (15) are investigated below.

C. Stability of the Tracking Error without Disturbances

The system (15) can be treated as two homogeneous subsystems and the term $\delta = \delta(\dot{r}^*, \omega^*, u_r, u_\theta, e_\theta, d_1, d_2)$ defines an interconnection of these systems. For $\delta = 0$, the system (15) is \mathbf{d} -homogeneous with degree μ . Since δ_2 is independent of ζ then stability and robustness properties of

the subsystems can be analyzed based on ISS of the cascade systems (see Appendix and [30], [31] and [32]).

Theorem 1: Let $d_1 = d_2 = 0$ and the control inputs, i.e., v and ω , for the system (1) be defined by (6), (8), (12) and (14). Let $\varepsilon < \min\{(2\sqrt{(1-\mu)k_1})/(2-\mu), 4k_1 k_2/(4k_1 + k_2)\}$. If $\sup_{t \in \mathbb{R}_+} \|\dot{r}^*(t)\| = \bar{v} < +\infty$ and $\omega^* \in L_{loc}^1$; then, the error system (15) is: 1) Globally Finite-Time Stable, for $\nu < 0$ and $\mu < 0$; and 2) Globally Asymptotically Stable and Locally Exponentially Stable, for $\mu = \nu = 0$.

Proof: If $d_2 = 0$; then, the closed-loop orientation error subsystem is given by $\dot{e}_\theta = -\alpha |e_\theta|^\nu e_\theta$. The latter system is globally finite-time stable for $\nu < 0$ and globally exponentially stable for $\nu = 0$.

According to the definition of monotone dilation, $\varepsilon < (2\sqrt{(1-\mu)k_1})/(2-\mu)$ implies that $G_{\mathbf{d}} P + P G_{\mathbf{d}} \succ 0$. Now, let the canonical homogeneous norm $\|\zeta\|_{\mathbf{d}}$ be a Lyapunov function candidate for the position error subsystem. The time derivative of the canonical homogeneous norm, for the disturbance-free system, is given by (2), hence

$$\frac{d\|\zeta\|_{\mathbf{d}}}{dt} = \frac{\partial \|\zeta\|_{\mathbf{d}}}{\partial e} f_1(\zeta) + \frac{\partial \|\zeta\|_{\mathbf{d}}}{\partial \zeta} [\delta_1^\top, \mathbf{0}^\top]^\top.$$

Let $s = \ln \|\zeta\|_{\mathbf{d}}$; then, we have that

$$\frac{\partial \|\zeta\|_{\mathbf{d}}}{\partial \zeta} f_1(\zeta) = \|\zeta\|_{\mathbf{d}} \frac{(\mathbf{d}(-s)\zeta)^\top P \mathbf{d}(-s) f_1(\zeta)}{(\mathbf{d}(-s)\zeta)^\top (P G_{\mathbf{d}}) \mathbf{d}(-s)\zeta},$$

and

$$\begin{aligned} & (\mathbf{d}(-s)\zeta)^\top P \mathbf{d}(-s) f_1(\zeta) \\ &= \begin{bmatrix} \|\zeta\|_{\mathbf{d}}^{\mu-1} e_r \\ \|\zeta\|_{\mathbf{d}}^{-1} u \end{bmatrix}^\top \begin{bmatrix} k_1 I_2 & \varepsilon I_2 \\ \varepsilon I_2 & I_2 \end{bmatrix} \begin{bmatrix} \|\zeta\|_{\mathbf{d}}^{\mu-1} u \\ \|\zeta\|_{\mathbf{d}}^{2\mu-1} k_1 e_r + \|\zeta\|_{\mathbf{d}}^{\mu-1} k_2 u \end{bmatrix} \\ &= -\|\zeta\|_{\mathbf{d}}^{3\mu-2} \varepsilon k_1 e_r^\top e_r - \|\zeta\|_{\mathbf{d}}^{2(\mu-1)} \varepsilon k_2 e_r^\top u \\ & \quad + \|\zeta\|_{\mathbf{d}}^{\mu-2} (\varepsilon - k_2) u^\top u \\ &= \|\zeta\|_{\mathbf{d}}^\mu (\mathbf{d}(-s)\zeta)^\top W \mathbf{d}(-s)\zeta, \end{aligned}$$

$$\text{with } W = \begin{bmatrix} -\varepsilon k_1 I_2 & -\frac{1}{2} \varepsilon k_2 I_2 \\ -\frac{1}{2} \varepsilon k_2 I_2 & (\varepsilon - k_2) I_2 \end{bmatrix}.$$

Then, $\varepsilon < 4k_1 k_2 / (4k_1 + k_2)$ implies that $W \prec 0$. Now, for $\delta_1 \neq 0$, we have that

$$\frac{\partial \|\zeta\|_{\mathbf{d}}}{\partial \zeta} [\delta_1^\top, \mathbf{0}^\top]^\top = \|\zeta\|_{\mathbf{d}} \frac{(\mathbf{d}(-s)\zeta)^\top P \mathbf{d}(-s) [\delta_1^\top, \mathbf{0}^\top]^\top}{(\mathbf{d}(-s)\zeta)^\top (P G_{\mathbf{d}}) \mathbf{d}(-s)\zeta}. \quad (16)$$

By definition, $\zeta^\top \mathbf{d}(-s) P \mathbf{d}(-s) \zeta = 1$, and using the Cauchy-Schwarz inequality, it yields

$$\frac{d\|\zeta\|_{\mathbf{d}}}{dt} \leq -\rho \|\zeta\|_{\mathbf{d}}^{1+\mu} + \frac{2\|\zeta\|_{\mathbf{d}} \|X^{-1/2} \mathbf{d}(-s) [\delta_1^\top, \mathbf{0}^\top]^\top\|_2}{\lambda_{\min}(X^{-1/2} G_{\mathbf{d}} X^{1/2} + X^{1/2} G_{\mathbf{d}}^\top X^{-1/2})},$$

where $\rho = 2 \frac{-\lambda_{\max}(P^{-0.5} W P^{-0.5})}{\lambda_{\max}(P^{0.5} G_{\mathbf{d}} P^{-0.5} + P^{-0.5} G_{\mathbf{d}} P^{0.5})}$. For the position tracking error subsystem, the dilation generator $G_{\mathbf{d}}$ is a diagonal matrix. Then, $\|P^{1/2} \mathbf{d}(-s) [\delta_1^\top, \mathbf{0}^\top]^\top\|_2 \leq \sqrt{\lambda_{\max}(P)} \|\mathbf{d}(-s) [\delta_1^\top, \mathbf{0}^\top]^\top\|_2$, and

$$\begin{aligned} \frac{d\|\zeta\|_{\mathbf{d}}}{dt} &\leq -\rho \|\zeta\|_{\mathbf{d}}^{1+\mu} + c \|\zeta\|_{\mathbf{d}} \|\mathbf{d}(-s) [\delta_1^\top, \mathbf{0}^\top]^\top\|_2 \\ &= -\rho \|\zeta\|_{\mathbf{d}}^{1+\mu} + c \|\zeta\|_{\mathbf{d}}^\mu \|\delta_1\|_2, \end{aligned}$$

where $c = \frac{2\sqrt{\lambda_{\max}(P)}}{\lambda_{\min}(P^{1/2} G_{\mathbf{d}} P^{-1/2} + P^{-1/2} G_{\mathbf{d}}^\top P^{1/2})}$. Using Lemma 2

and (10) with $\hat{d}_1 = 0$, we derive

$$\begin{aligned} \frac{d\|\zeta\|_{\mathbf{d}}}{dt} &\leq -\rho \|\zeta\|_{\mathbf{d}}^{1+\mu} + 2c \|e\zeta\|_{\mathbf{d}}^\mu (\bar{v} + \frac{\|\zeta\|_{\mathbf{d}}}{\sqrt{\lambda_{\min}(P)}}) \left| \sin \frac{e_\theta}{2} \right| \\ &= -\|\zeta\|_{\mathbf{d}}^{1+\mu} \left(\rho - \frac{2c \left| \sin \frac{e_\theta}{2} \right|}{\sqrt{\lambda_{\min}(P)}} \right) + 2c \bar{v} \|\zeta\|_{\mathbf{d}}^\mu \left| \sin \frac{e_\theta}{2} \right|. \quad (17) \end{aligned}$$

For the position tracking error subsystem, the obtained inequality guarantees: the absence of the finite-time blow-up for $\mu \leq 0$; the ISS of the position tracking error subsystem with respect to small input e_θ .

Moreover, if $\delta_1 = 0$, then the position error subsystem is finite-time stable for $\mu < 0$; subsequently, the entire system is finite-time stable, taking into account the cascade structure and the finite-time stability of the orientation subsystem for $\nu < 0$. For $\nu = \mu = 0$, using Theorem 2 from [31], we conclude integral ISS (iISS) of the first subsystem with respect to e_θ . Together with ISS for the small inputs, this guarantees that the first subsystem is strongly iISS⁴, and by Corollary 2, the cascade system is globally asymptotically stable. Local exponential stability comes from the estimate (17) with $\mu = 0$. ■

D. Robustness Analysis

As illustrated in Section IV-A, when $d_1 = d_2 = 0$, the term δ_1 depends on the virtual control u_r^* and the derivative of the trajectory \dot{r}^* , and it is vanishing as the orientation error e_θ reaching zero. For $d_1 \neq 0$ and $d_2 \neq 0$, δ_1 is not vanishing as e_θ reaches zero, so the system is highly coupled. In this section, the behavior of the system (15), with $d_1 \neq 0$ and $d_2 \neq 0$, is analyzed based on ISS.

Theorem 2: *Let conditions of Theorem 1 be satisfied, for $-1 \leq \nu < \mu \leq 0$. If $\sup_{t \in \mathbb{R}_+} \|\dot{r}^*\| = \bar{v} < +\infty$ and $\sup_{t \in \mathbb{R}_+} \|\omega^*\| = \bar{\omega}^* < +\infty$; then, for any given μ , there exist k_1 and k_2 such that the tracking error system (15) is ISS with respect to $d_i \in [-\hat{d}_i, \hat{d}_i]$, $\hat{d}_i \in (0, 1)$, $i = 1, 2$.*

Proof: Let $-1 \leq \nu < \mu \leq 0$. For the orientation tracking error subsystem, we have

$$\dot{e}_\theta = -\alpha|e_\theta|^\nu e_\theta + d_2(-\alpha|e_\theta|^\nu e_\theta + \omega^*). \quad (18)$$

Taking the candidate Lyapunov function $V_1 = \frac{1}{2}e_\theta^2$, we derive

$$\begin{aligned} \dot{V}_1 &= -(d_2 + 1)\alpha|e_\theta|^\nu e_\theta^2 + d_2\omega^* e_\theta \\ &\leq -|e_\theta| \left((1 - |d_2|)\alpha|e_\theta|^{1+\nu} - |d_2|\|\omega^*\| \right). \end{aligned} \quad (19)$$

Hence, the orientation tracking error subsystem is ISS with respect to $|d_2| \leq \hat{d}_2 < 1$. In addition, the orientation error can converge to a neighbourhood of origin:

$$\limsup_{t \rightarrow +\infty} |e_\theta(t)| \leq \left(\frac{\hat{d}_2 \bar{\omega}^*}{(1 - \hat{d}_2)\alpha} \right)^{1/(1+\nu)}. \quad (20)$$

Considering the position tracking error subsystem with disturbance, using Lemma 2, we derive

$$\begin{aligned} \frac{d}{dt} \|\zeta\|_a &\leq -\rho \|\zeta\|_a^{1+\mu} + c \|\zeta\|_a^\mu \|\delta_1\|_2 \\ &\leq -\|\zeta\|_a^{1+\mu} \left(\rho - \frac{2c(1 + \hat{d}_1) \left| \sin\left(\frac{e_\theta}{2}\right) \right| + c\hat{d}_1}{\sqrt{\lambda_{\min}(P)}} \right) \\ &\quad + \|\zeta\|_a^\mu \left(2c(1 + \hat{d}_1) \left| \sin\left(\frac{e_\theta}{2}\right) \right| + c\hat{d}_1 \right) \bar{v}. \end{aligned} \quad (21)$$

The above inequality implies the position tracking error subsystem is ISS with respect to small e_θ and d_1 , and the system has no finite-time blow-up since $\mu \leq 0$. Taking into

⁴A system $\dot{x} = f(x)$, $x(0) = x_0$ is said to be Strongly iISS if it is both iISS, and ISS with respect to small inputs (for more details, please see [33]).

account the cascade structure, we conclude that the whole error system is ISS with respect to small d_1 and d_2 . ■

Notice that, P and G_d are functions of k_1 , ε and μ , but W is determined by (μ, k_1, ε) in addition to k_2 . Then, for fixed k_1 , ε and μ , the matrix W is function of k_2 and it follows that

$$\lambda_{\max}(P^{-0.5}WP^{-0.5}) = \left(\varepsilon + \frac{k_2}{2}\right) \left(\frac{k_1}{k_1 - \varepsilon^2}\right)^{1/2} - \frac{k_2}{2}.$$

Therefore, for a sufficiently small $\varepsilon >$, it is clear that $k_2 \rightarrow \infty$ implies that $\lambda_{\max}(P^{-0.5}WP^{-0.5}) \rightarrow -\infty$. Thus, there exists a sufficient large k_2 such that $\rho > (c(2 + 3d_1))/\sqrt{\lambda_{\min}(P)}$; and then, the proof is complete.

As proven in Theorem 1, for the disturbed system, given any μ, ν and positive k_1, k_2, α , there exists a sufficiently small ε such that the disturbance-free system is asymptotically stable. To ensure the robustness of the controller with respect to slippage, an increase in the value of k_2 is necessary. The parameter α in (14) defines the magnitude of the stabilization error for the orientation subsystem. Using the estimates \hat{d}_1 and \hat{d}_2 of the perturbations d_1 and d_2 , respectively, the parameter α can be selected such that the closed-loop becomes practically stable. The following corollary describes such a result.

Corollary 1: *Let conditions of Theorem 2 hold. If $\hat{d}_1 < 1$ and $\hat{d}_2 < 1$; then, there exist sufficiently large α and k_2 , such that the tracking error system (15) is practically stable:*

$$\limsup_{t \rightarrow +\infty} |e_\theta(t)| \leq \left(\frac{\hat{d}_2 \bar{\omega}^*}{(1 - \hat{d}_2)\alpha} \right)^{1/(1+\nu)}, \quad (22)$$

$$\limsup_{t \rightarrow +\infty} \|e_r(t)\|_2 \leq \frac{1}{\sqrt{\lambda_{\min}(P)}} \left(\frac{\bar{v}}{\underline{\chi}} \right)^{(1-\mu)}, \quad (23)$$

with $\underline{\chi} = \rho c \left(2(1 + \hat{d}_1) \left(\frac{\hat{d}_2 \bar{\omega}^*}{(1 - \hat{d}_2)\alpha} \right)^{1/(1+\nu)} - \hat{d}_1 \right)^{-1} - \frac{c}{\sqrt{\lambda_{\min}(P)}}$.

Proof: From (20), we derive

$$\limsup_{t \rightarrow +\infty} |e_\theta(t)| \leq \left(\frac{\hat{d}_2 \bar{\omega}^*}{(1 - \hat{d}_2)\alpha} \right)^{1/(1+\nu)} = \bar{e}_\theta.$$

Since $2|\sin(e_\theta/2)| \leq |e_\theta|$; then, starting from some instant of time, we have $\rho - \left(2c(1 + \hat{d}_1)\bar{e}_\theta + c\hat{d}_1 \right) / \sqrt{\lambda_{\min}(P)} > 0$; and then, using (21) and (26), we complete the proof. ■

The latter corollary implies that the tracking error system can be stabilized to an arbitrarily small neighbourhood of the origin by tuning the parameters α, k_1 and k_2 provided that $\nu < 0$ and $\mu < 0$. Indeed, the larger α less the orientation error (see (20)) and the larger k_1 and k_2 , better the accuracy of the position tracking (see (23)).

The tuning process can be carried out in a straightforward manner by utilizing the values of α, k_1 , and k_2 to determine the limit set of the tracking error, with k_2 serving as a damping gain to mitigate the effects of slippage. The implementation issues of the proposed control law are summarized in Algorithm 1.

Algorithm 1 Homogeneous control for UMR

- 1: *Input:* r, θ, r^*, θ^*
 - 2: *Initialization:* Select $-1 \leq \nu \leq 0, -1 \leq \mu \leq 0, \alpha > 0$, and $u_r(0) = \mathbf{0}$.
 - 3: *Control:* Compute $v = |\dot{r}^* + u_r|_2$ and $\omega = \omega^* - \alpha|\theta - \theta^*|^\nu(\theta - \theta^*)$, where u_r is given by (12) and ω^* is given by (7).
 - 4: *Tuning parameters:* Begin with a small ε and k_2 , then select an appropriate k_1 based on the range of velocity allowed by the vehicle. Choose α , and increase k_2 , according to (22) and (23).
-

V. EXPERIMENTAL RESULTS

The experimental results are obtained using the QBot2 platform by Quanser (see Fig. 2). The QBot2 possesses a processing embedded system, which communicates through a real-time control software called QUARC with a sampling time equal to 1[ms]. Such software allows us to build a direct interface with Matlab-Simulink and build different algorithms and controllers. The QBot2 posture and orientation are obtained through odometry, *i.e.*, the wheel spinning is measured by the robot encoders and through the kinematic model of the UMR, we can compute the total displacement and orientation angle. Note that the linear and angular velocities are the control inputs.



Fig. 2: QBot2 by Quanser

The initial conditions for the kinematics are $x(0) = 0.5$ [m], $y(0) = 0$ [m] and $\theta(0) = 0$ [rad]. For the experimental results, we select $r^*(t) = r_d(t)$. Then, the desired trajectory is given by $\omega_d(t) = (\dot{x}_d\ddot{y}_d - \dot{y}_d\ddot{x}_d)/(\dot{x}_d^2 + \dot{y}_d^2)$, $v_d(t) = \sqrt{\dot{x}_d^2 + \dot{y}_d^2}$, $x_d(t) = \cos(0.13t)$, $y_d(t) = \sin(0.26t)$ and $\theta_d(t) = \int_0^t \omega_d(\tau)d\tau$; and hence, one has that $\bar{w}^* = 0.1560$. For robustness purposes, in addition to the intrinsic disturbances that the experimental platform possesses (*e.g.*, the effect of the difference between the angular velocity of the wheel and the linear input velocity v , caused by the wheel slipping on the surface; or the rate deviation of the change of the orientation angle θ due to the wheel slippage), some external signals, added by software, are considered. The external perturbations are taken as $d_1(t) = 0.01 \sin(t) + 0.01$ and $d_2(t) = 0.03 \cos(t) + 0.03$; and then, $\hat{d}_1 = 0.02$ and $\hat{d}_2 = 0.06$. Moreover, as one can see in Fig. 2, we have

added some soil on the surface to try to induce some slipping effect between the wheels and the surface.

Then, the parameters of the proposed homogeneous controller (HC) are selected, based on Algorithm 1, *i.e.*, based on the conditions of Theorem 2 and Corollary 1, as $\mu = -0.5$, $\nu = -0.6$, $\alpha = 3$, $k_1 = 2.5$, $k_2 = 3$ and $\varepsilon = 0.2$. Note that the conditions of Corollary 1 hold since $\varepsilon = 0.8696 < \min\{2\sqrt{(1-\mu)k_1}/(2-\mu), 4k_1k_2/(4k_1+k_2)\} = \min\{1.5492, 2.3077\}$, $\hat{d}_1 = 0.02 < 1$ and $\hat{d}_2 = 0.06 < 1$.

In order to illustrate the performance of the proposed controller, we compare it with two controllers, *i.e.*, a first-order sliding-mode (FOSM) controller proposed in [6] and a nonlinear controller (NC) proposed by [34]. The FOSM controller is given as $v = v_d(t) \cos(e_3) + \rho_1 \text{sign}(s_1)$, $\omega = \omega_d(t) + \rho_2 \text{sign}(s_2)$, where $s_1 = e_1$, $s_2 = e_3 + \arcsin(\min\{\delta_1|e_2|^{-1}, \delta_2\}e_2)$, $e_1 = \cos(\theta)(x_d - x) + \sin(\theta)(y_d - y)$, $e_2 = \cos(\theta)(y_d - y) - \sin(\theta)(x_d - x)$, $e_3 = \theta_d - \theta$, with $\rho_1 = 0.04$, $\rho_2 = 0.45$, $\delta_1 = 0.3$ and $\delta_2 = 6$. The NC has the following form $v = v_d(t) \cos(e_3) + \rho_1 e_1$, $\omega = \omega_d(t) + \rho_3 e_3 + v_d(t)\rho_2 e_2 \sin(e_3)/e_3$, with $\rho_1 = 2$, $\rho_2 = 2$ and $\rho_3 = 1.5$.

The three controllers have been tuned in order to obtain the best possible trajectory-tracking performance. The results are shown in Figs. 3, 4 and 5. In Fig. 3, we can see that the proposed HC provides an outstanding trajectory-tracking performance similar to the FOSM controller despite the intrinsic disturbances and the considered external perturbations, without overshoots. On the other hand, the NC presents some problems in tracking the desired trajectory showing a considerable overshoot. The control signals are illustrated in Fig. 4 and we can see that the HC and the NC use similar control efforts but the FOSM controller requires a more aggressive control signal and has chattering. The velocity difference between the control input and the current measurements illustrates the slippage-effect. On the other hand, Fig. 5 illustrates the norm of the trajectory tracking error for each controller, indicating that the addition of soil results in a tracking error increment.

To better analyze the performance of the controllers in terms of tracking error and control effort, we provide the mean value of the performance indexes $e_{rms}(t) = (\frac{1}{T} \int_{t-T}^t \|\bar{e}(\tau)\|^2 d\tau)^{1/2}$ and $u_{rms}(t) = (\frac{1}{T} \int_{t-T}^t \|u(\tau)\|^2 d\tau)^{1/2}$, with $\bar{e} = [x - x_d, y - y_d, \theta - \theta_d]^\top$, $\bar{u} = [\omega, v]^\top$, and $T = 0.1$. We evaluated the mean value of $e_{rms}(t)$ for $t \in [40, 60]$, which is the steady-state performance, and the maximum value of $\|\bar{e}(t)\|$ for $t \in [0, 20]$, which is the transient performance. These metrics are presented in Table I. The results show that the HC outperforms the FOSM and the NC, respectively, in the trajectory-tracking performance with less control effort. Moreover, the FOSM exhibits the least steady-state error but the largest error during the transient phase, while the NC method had the largest steady-state error but the least error during the transient phase. These results validate that the proposed HC provides a better balance between steady-state

TABLE I: Performance Indexes

Index	HC	FOSM	NC
$e_{rms}(t), t \in [0, 60]$	0.0562	0.18898	0.1471
$u_{rms}(t), t \in [0, 60]$	0.3988	0.5282	0.4445
$e_{rms}(t), t \in [40, 60]$	0.0488	0.0328	0.1228
$max\ \bar{e}(t)\ , t \in [0, 20]$	0.5063	0.6763	0.5017

error and transient performance.⁵

VI. CONCLUSIONS

This paper proposes a family of homogeneous controllers to address the trajectory-tracking problem in perturbed UMRs. The controllers demonstrate global finite-time and asymptotic stability in the absence of perturbations. Stability analysis is simplified using the cascade structure and strongly iISS when $\nu = \mu = 0$. The controllers guarantee ISS with respect to small perturbations d_1 and d_2 , with tracking error precision dependent on the perturbation magnitudes and control parameters. Real-time experiments with the wheeled mobile robot QBot2 by Quanser illustrate the controller's trajectory-tracking performance and robustness properties.

APPENDIX

Consider a cascade system

$$\dot{x}_1 = f_1(x_1, x_2), \quad \dot{x}_2 = f_2(x_2), \quad (24)$$

where $f_1 : \mathbb{R}^{n_1} \times \mathbb{R}^{n_2} \rightarrow \mathbb{R}^{n_1}$ and $f_2 : \mathbb{R}^{n_2} \times \mathbb{R}^{m_2} \rightarrow \mathbb{R}^{n_2}$ denote two locally Lipschitz functions satisfying $f_1(0, 0) = 0$ and $f_2(0, 0) = 0$.

Corollary 2: [35]. *If the system $\dot{x}_1 = f_1(x_1, x_2)$ is Strongly iISS and the origin of $\dot{x}_2 = f_2(x_2)$ is globally asymptotically stable, then the origin of the cascade (24) is globally asymptotically stable.*

Then, the following lemma is an auxiliary result used in the proofs of Theorems 1 and 2.

Lemma 2: *For the position tracking error subsystem with the control defined as (12), δ_1 is bounded by*

$$\|\delta_1\|_2 \leq 2(1 + \hat{d}_1)(\bar{v} + \frac{\|\zeta\|_d}{\sqrt{\lambda_{\min}(P)}}) \left| \sin\left(\frac{e_\theta}{2}\right) \right| + \hat{d}_1(\bar{v} + \frac{\|\zeta\|_d}{\sqrt{\lambda_{\min}(P)}}). \quad (25)$$

Proof: By definition of the canonical homogeneous norm, we have $\|\mathbf{d}(-\ln \|\zeta\|_d)\zeta\| = 1$. Hence, we derive

$$\|\zeta\|_d^{-2(1-\mu)} e_r^\top e_r + \|\zeta\|_d^{-2} u_r^\top u_r \leq \frac{1}{\lambda_{\min}(P)}. \quad (26)$$

Then, it yields that $\|u_r\| \leq \|\zeta\|_d / \sqrt{\lambda_{\min}(P)}$. The proof is complete by taking into account (6) and (10). ■

ACKNOWLEDGEMENT

This work was supported in part by the SEP-CONACYT-ANUIES-ECOS NORD Project 315597 and ECOS NORD Project M20M04. Y. Zhou acknowledges the support of CSC Grant 202006030019, China. H. Ríos was supported in part by CONACYT CVU 270504 Project 922, and in part by TecNM Projects. M. Mera was supported in part by

⁵A YouTube video, showing these experimental results, may be watched at the following link <https://youtu.be/JpW9Z07JN4k>.

Project IPN-SIP 20230170. Andrey Polyakov acknowledges the support of the National Natural Science Foundation of China under Grant 62050410352.

REFERENCES

- [1] G. Campion, G. Bastin, and B. D'Andreá-Novel. Structural properties and classification of kinematic and dynamic models of wheeled mobile robots. *IEEE Transactions on Robotics and Automation*, 12(1):47–62, 1996.
- [2] D. Wang and C. B. Low. Modeling and analysis of skidding and slipping in wheeled mobile robots: Control design perspective. *IEEE Transactions on Robotics*, 24(3):676–687, 2008.
- [3] S.J. Yoo. Adaptive tracking control for a class of wheeled mobile robots with unknown skidding and slipping. *IET Control Theory & Applications*, 4(10):2109–2119, 2010.
- [4] H. Gao, X. Song, L. Ding, K. Xia, N. Li, and Z. Deng. Adaptive motion control of wheeled mobile robot with unknown slippage. *International Journal of Control*, 87(8):1513–1522, 2014.
- [5] C. Chen, H. Gao, L. Ding, W. Li, H. Yu, and Z. Deng. Trajectory tracking control of wms with lateral and longitudinal slippage based on active disturbance rejection control. *Robotics and Autonomous Systems*, 107:236–245, 2018.
- [6] M. Mera, H. Ríos, and E. A. Martínez. A sliding-mode based controller for trajectory tracking of perturbed unicycle mobile robots. *Control Engineering Practice*, 102:104548, 2020.
- [7] P. Rochel, H. Ríos, M. Mera, and A. Dzul. Trajectory tracking for uncertain unicycle mobile robots: A super-twisting approach. *Control Engineering Practice*, 122:105078, 2022.
- [8] S. Wei, K. Uthachana, M. Žefran, and R. DeCarlo. Hybrid model predictive control for the stabilization of wheeled mobile robots subject to wheel slippage. *IEEE Transactions on Control Systems Technology*, 21(6):2181–2193, 2013.
- [9] Y. Hong. H_∞ control, stabilization, and input-output stability of non-linear systems with homogeneous properties. *Automatica*, 37(6):819–829, 2001.
- [10] S. P. Bhat and D. S. Bernstein. Geometric homogeneity with applications to finite-time stability. *Mathematics of Control, Signals and Systems*, 17(2):101–127, 2005.
- [11] V. Andrieu, L. Praly, and A. Astolfi. Homogeneous Approximation, Recursive Observer Design, and Output Feedback. *SIAM Journal of Control and Optimization*, 47(4):1814–1850, 2008.
- [12] A. Polyakov. *Generalized homogeneity in systems and control*. Springer, 2020.
- [13] S. Kimura, H. Nakamura, and Y. Yamashita. Control of two-wheeled mobile robot via homogeneous semiconcave control lyapunov function. *IFAC Proceedings Volumes*, 46(23):92–97, 2013.
- [14] S. Kimura, H. Nakamura, and Y. Yamashita. Asymptotic stabilization of two-wheeled mobile robot via locally semiconcave generalized homogeneous control lyapunov function. *SICE Journal of Control, Measurement, and System Integration*, 8(2):122–130, 2015.
- [15] R. T. M'Closkey and R. M. Murray. Convergence rates for nonholonomic systems in power form. In *1993 American Control Conference*, pages 2967–2972, 1993.
- [16] R. T. M'Closkey and R. M. Murray. Nonholonomic systems and exponential convergence: some analysis tools. In *Proceedings of 32nd IEEE Conference on Decision and Control*, pages 943–948, 1993.
- [17] J. Godhavn and O. Egeland. Lyapunov-based time varying control for exponential stabilization of a unicycle. *IFAC Proceedings Volumes*, 29(1):2454–2459, 1996.
- [18] R. T. M'Closkey and R. M. Murray. Exponential stabilization of driftless nonlinear control systems using homogeneous feedback. *IEEE Transactions on Automatic Control*, 42(5):614–628, 1997.
- [19] S. Kimura, T. Nakai, H. Nakamura, T. Ibuki, and M. Sampei. Finite-time control of two-wheeled mobile robot via generalized homogeneous locally semiconcave control lyapunov function. In *2016 55th Annual Conference of the Society of Instrument and Control Engineers of Japan (SICE)*, pages 1643–1648. IEEE, 2016.
- [20] D. Wu, Y. Cheng, H. Du, W. Zhu, and M. Zhu. Finite-time output feedback tracking control for a nonholonomic wheeled mobile robot. *Aerospace Science and Technology*, 78:574–579, 2018.
- [21] S. Li and Y-P Tian. Finite-time stability of cascaded time-varying systems. *International Journal of Control*, 80(4):646–657, 2007.

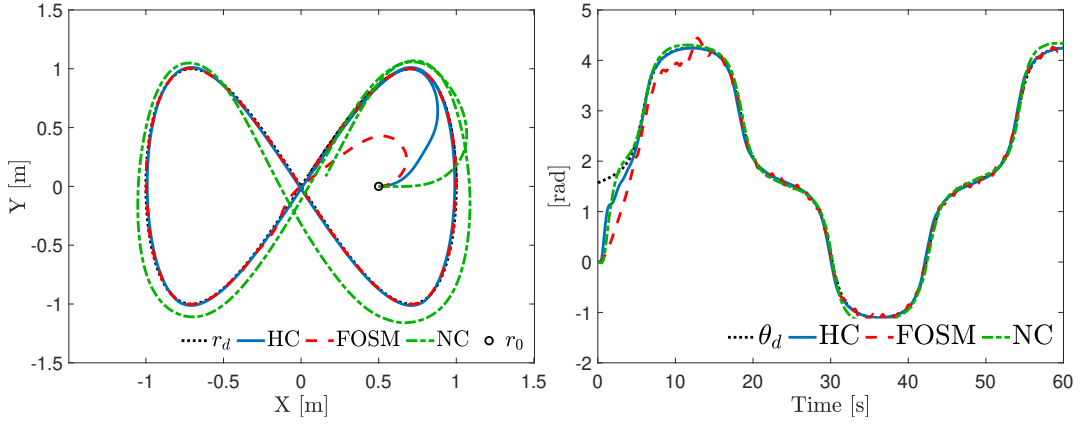


Fig. 3: Experimental Results for System Trajectories

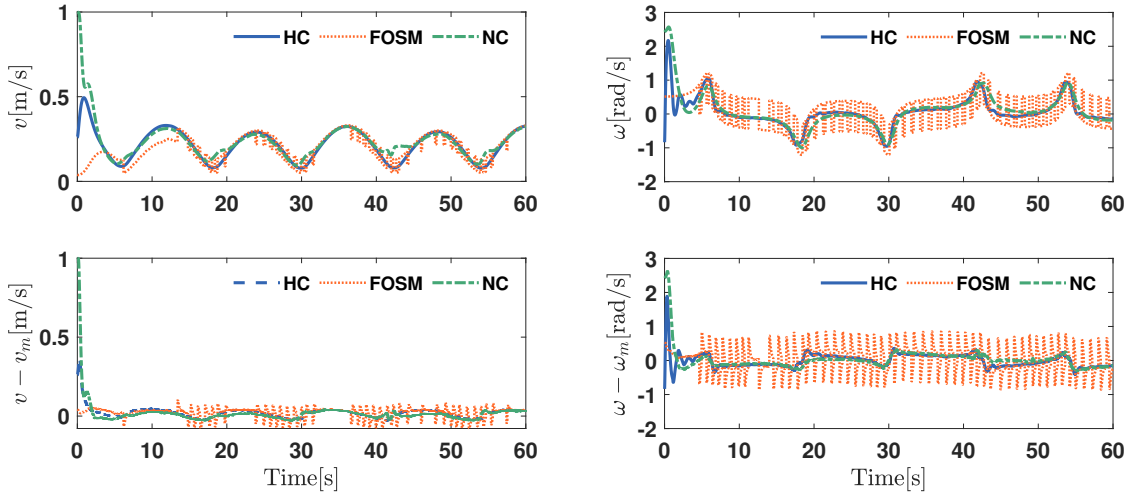


Fig. 4: Experimental Results for Control Signals. Signals v_m and ω_m are from current measurements.

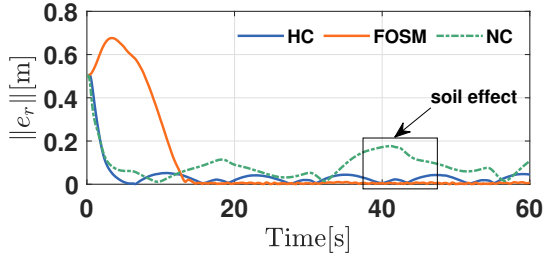


Fig. 5: Norm of the Trajectory Tracking Error

[22] S. Ding, S. Li, and Q. Li. Global uniform asymptotical stability of a class of nonlinear cascaded systems with application to a nonholonomic wheeled mobile robot. *International Journal of Systems Science*, 41(11):1301–1312, 2010.

[23] S. Ding and W. X. Zheng. Global stabilisation of a class of generalised cascaded systems by homogeneous method. *International Journal of Control*, 89(4):815–832, 2016.

[24] A. Polyakov, J.-M. Coron, and L. Rosier. On homogeneous finite-time control for linear evolution equation in hilbert space. *IEEE Transactions on Automatic Control*, 63(9):3143–3150, 2018.

[25] A. Polyakov. Sliding mode control design using canonical homogeneous norm. *International Journal of Robust and Nonlinear Control*, 29(3):682–701, 2019.

[26] Y. Zhou, H. Ríos, M. Mera, A. Polyakov, G. Zheng, and A. Dzul. Trajectory tracking in unicycle mobile robots: A homogeneity-based control approach. In *The 22nd World Congress of the International Federation of Automatic Control IFAC World Congress*, 2023.

[27] L. Rosier. Homogeneous Lyapunov function for homogeneous continuous vector field. *Systems & Control Letters*, 19:467–473, 1992.

[28] L.S. Husch. Topological characterization of the dilation and the translation in frechet spaces. *Mathematische Annalen*, 190(1):1–5, 1970.

[29] V.I. Zubov. On systems of ordinary differential equations with generalized homogeneous right-hand sides. *Izvestia vuzov. Mathematica (in Russian)*, 1:80–88, 1958.

[30] E. D. Sontag. Smooth stabilization implies coprime factorization. *IEEE Transactions on Automatic Control*, 34(4):435–443, 1989.

[31] E. D. Sontag. Comments on integral variants of ISS. *Systems & Control Letters*, 34(1-2):93–100, 1998.

[32] D. Angeli, E.D. Sontag, and Y. Wang. A characterization of integral input-to-state stability. *IEEE Transactions on Automatic Control*, 45(6):1082–1097, 2000.

[33] A. Chaillet, D. Angeli, and H. Ito. Combining iISS and ISS with respect to small inputs: the strong iISS property. *IEEE Transactions on Automatic Control*, 59(9):2518–2524, 2014.

[34] M. Maghenem, A. Loría, and E. Panteley. Formation-tracking control of autonomous vehicles under relaxed persistency of excitation conditions. *IEEE Transactions on Control Systems Technology*, 26(5):1860–1865, 2017.

[35] A. Chaillet, D. Angeli, and H. Ito. Strong iISS is preserved under cascade interconnection. *Automatica*, 50(9):2424–2427, 2014.